Site directed spin labelling and pulsed dipolar electron paramagnetic resonance (double electron–electron resonance) of force activation in muscle

2005 J. Phys.: Condens. Matter 17 S1459

(http://iopscience.iop.org/0953-8984/17/18/004)

INSTITUTE OF PHYSICS PUBLISHING JOURNAL OF PHYSICS: CONDENSED MATTER

J. Phys.: Condens. Matter **17** (2005) S1459–S1469 doi:10.1088/0953-8984/17/18/004

Site directed spin labelling and pulsed dipolar electron paramagnetic resonance (double electron–electron resonance) of force activation in muscle

Piotr G Fajer

Institute of Molecular Biophysics, Department of Biological Science, National High Magnetic Field Laboratory, Florida State University, Tallahassee, FL 32310, USA

E-mail: fajer@magnet.fsu.edu

Received 9 December 2004
Published 22 April 2005
Online at stacks.iop.org/JPhysCM/17/S1459

Abstract

The recent development of site specific spin labelling and advances in pulsed electron paramagnetic resonance (EPR) have established spin labelling as a viable structural biology technique. Specific protein sites or whole domains can be selectively targeted for spin labelling by cysteine mutagenesis. The secondary structure of the proteins is determined from the trends in EPR signals of labels attached to consecutive residues. Solvent accessibility or label mobility display periodicities along the labelled polypeptide chain that are characteristic of β-strands (periodicity of 2 residues) or α-helices (3.6 residues). Low-resolution 3D structure of proteins is determined from the distance restraints. Two spin labels placed within 60–70 Å of each other create a local dipolar field experienced by the other spin labels. The strength of this field is related to the interspin distance, $\propto r^{-3}$. The dipolar field can be measured by the broadening of the EPR lines for the short distances (8–20 Å) or for the longer distances (17–70 Å) by the pulsed EPR methods, double electron–electron resonance (DEER) and double quantum coherence (DQC). A brief review of the methodology and its applications to the multisubunit muscle protein troponin is presented below.

(Some figures in this article are in colour only in the electronic version)

1. Introduction

The last decade witnessed the rapid development of structural methods resulting in a nearly exponential increase of solved protein structures. Attention is now shifting from structure determination as a goal in itself towards a description of the structural changes that facilitate the function of biological macromolecules. This new goal has created an increasing need for methods that extend and complement the high resolution static structures of isolated proteins

in crystals to descriptions of proteins in solution and in large macromolecular complexes that are functionally active. Furthermore, the increasing realization of the significance of structural heterogeneity and the order-to-disorder transitions in many biological processes gives a premium to methods that are sensitive to structural heterogeneity and disorder. Equally important is the addition of time resolution to structural methods so that protein dynamics and/or structural transitions accompanying biological activity are captured.

Fluorescence spectroscopy is one of these techniques. It has unparalleled sensitivity that allows the observation of single molecules in real time; it is sensitive to rotational and translational diffusion and capable of measuring distances between fluorophores. Electron paramagnetic resonance (EPR or ESR) spectroscopy shares many of the advantages of fluorescence methods. Not quite as sensitive, it has the advantages of simpler protein chemistry and spectral resolution of orientations as each position in the EPR spectrum corresponds to a well defined orientation of the spin with respect to the magnetic field. This paper reviews briefly the emerging EPR methods for structural biology and shows their application to problems in muscle activation.

2. EPR methods in structural biology

2.1. Site directed spin labelling: mutagenesis and labelling

The pioneering work of Hubbell and collaborators (reviewed in [1–3]) combined the power of molecular biology and EPR spectroscopy. Previously EPR was limited to paramagnetic biomolecules such as metalloproteins or to proteins with a few naturally occurring cysteines to which paramagnetic probes (spin labels) could be selectively attached. By 1990 molecular biology afforded engineering of cysteines at targeted sites in proteins. The cysteine scanning method, where a whole stretch of the polypeptide chain is substituted with cysteines one residue at a time, is now quite common. Initially a labour intensive method, it has been greatly accelerated by automatic sequencing, affinity tags and even robotics—60 single-cysteine mutants can now be prepared within a couple of weeks. Proteins are bacterially expressed, modified with spin labels and purified on affinity columns. Figure 1 shows the labelling of a cysteine residue with MTSSL, a small spin label of the size of a tryptophan residue. Labelling of many proteins with this spin label has been shown to result in minimal structural perturbation and more importantly little functional perturbation [4].

The EPR signal is exquisitely sensitive to the local environment; it reports on the steric restriction experienced by the label and on the hydrophobicity of the media surrounding the label (table 1). Both are used to determine the local protein structure. The label mobility is determined by the steric restrictions imposed by neighbouring residues and by backbone motion. Labels on the protein surface, in loops between helices or β-strands or labels facing the protein interior or involved in subunit interfaces all display characteristic mobilities. As spin label mobility increases the EPR line width narrows—this motionally narrowed line width is used to identify the structure of the labelled domain. The exposure of spin labels to aqueous or membrane environment is measured by the accessibility of water/membrane soluble paramagnetic relaxation agents in a manner analogous to fluorescence quenching. For example, O_2 is more soluble in a hydrophobic milieu than in water, and will relax preferentially labels that are buried within a membrane or interior of a protein. Water soluble chelators of paramagnetic Ni^{2+}, ethylene diamine-*N*, *N*′-diacetic acid (NiEDDA), on the other hand, will relax water exposed residues. The efficiency of relaxation is proportional to the bimolecular collision rate and is measured by broadening of the spectrum with increasing power (power saturation) in the presence and absence of relaxing agent (table 1).

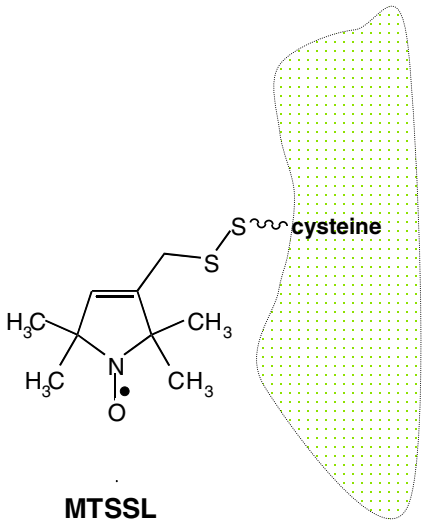

Figure 1. Spin label, nitroxide methyl-thiosulfonate (MTSSL) attached to a cysteine residue of a protein. The unpaired electron whose resonance is observed is located in the N–O bond.

Table 1. EPR methodologies for structural biology.

Molecular property		EPR	Signal	
Solvent accessibility	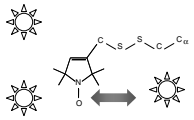	Power saturation	Amplitude	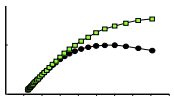
Mobility	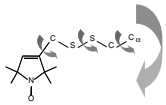	Conventional EPR	Splitting	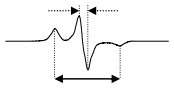
Spin–spin distance	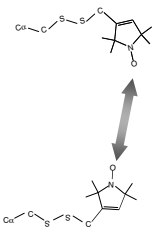	Dipolar EPR	Broadening	
		DEER, DQC	Echo modulation	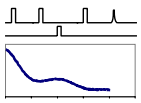

The trends in label mobility or water accessibility, as a function of spin label position along the chain, identify the secondary structure and its environment. β-strands that lie on the surface of membranes or form a surface of a protein display a two-residue periodicity, while α-helices display 3.6-residue periodicity. The secondary elements are often identified by the power Fourier transform of the accessibility/mobility trends which removes local site chain variations [4].

2.2. Dipolar EPR

2.2.1. Conventional. In addition to secondary structure identification, EPR is increasingly used to determine medium- and long-range distance constraints within the proteins. The analogous fluorescence method is fluorescence energy transfer (FRET). The magnetic dipole interaction between two spin labels placed at the sites of interest results in a small local magnetic field that broadens the spectrum. The extent of broadening in doubly labelled samples is obtained by comparison with the singly labelled protein (single-cysteine mutants); the ratio of the Fourier transforms of doubly and singly labelled spectra gives a broadening function that is proportional to the r^3 distance between the labels [5]. This method was shown to reproduce accurately the distances in synthetic peptides in the range between 8 and 20 Å. The drawback of this method is the necessity to freeze the samples. Ambient temperature is sensitive to r^6 of the interspin distance and is valid only for small proteins ($<$12 kD). Similar distances, 8–20 Å, have been measured in model systems [6].

2.2.2. Pulsed DEER. Pulsed EPR methods increase the range of distance sensitivity to $>$60 Å; however, they require specialized EPR spectrometers that only recently became commercially available. One of these methods, DEER (double electron–electron resonance) is depicted in figure 2 [7–9]. Three pulses at 'observation frequency' (ν_o) excite a subset of molecules with a particular orientation within an isotropic sample and generate an echo. A fourth, 'pumping' pulse with a different frequency (ν_p) excites a different subset of molecules and is applied between the 'observation' pulses. If the two populations are in physical proximity then the local magnetic field induced by the *pumped* molecules is sensed by the *observed* molecules. As the timing of the pumping pulse is varied, the echo amplitude is modulated with a periodicity related to the distance between the spins. Fourier transform of the echo modulation yields a 'Pake' pattern. The distance is directly calculated from the 'Pake' pattern splitting. The echo modulation shown in figure 2 is for a rigid biradical with a spin–spin separation of 37 Å (gift of G Jesch). The distance recovered from the Pake pattern is 36 Å. Freed and collaborators developed another pulsed method, DQC (double quantum coherence), that uses a single frequency [10]. This method requires a strong microwave amplifier that is not commercially available.

The DEER and DQC methods are sensitive to the distribution of distances. Figure 3 illustrates how the increasing distribution of the interspin distance decreases the modulation of the echo. The sensitivity to average distance is still preserved even in the presence of a wide distribution. The current limitation of these methods is that they rely on spin echoes and hence they have to be performed at low temperatures (80 K) at which the T_2 relaxation time is long enough to allow echo detection.

2.2.3. Pulsed saturation recovery. An entirely different EPR method measures distances between paramagnetic metals e.g. Ni^{2+}, Gd^{3+}, Cu^{2+} and the nitroxides. The spin–lattice relaxation time of metals is usually orders of magnitude shorter than that of nitroxides. If the nitroxide is within 60 Å of the metal, the dipolar interaction between the spins effectively enhances the rate of relaxation in a distance dependent manner [11]. Many proteins possess native metal sites that can ligand paramagnetic metals; for others one uses cysteine-directed derivatives of strong chelators such as 1,4,7,10-tetra-azacyclododecane-1,4,7,10-tetra-acetate (DOTA). Nitroxide spin relaxation is observed by inversion recovery or saturation recovery methods. Inversion recovery follows time evolution of an echo after a 180° pulse that inverts the signal, 180°–τ–90°–180° (figure 4). Saturation recovery uses pulses to saturate the spins and continuous wave EPR to observe the recovery of the signal in time. The

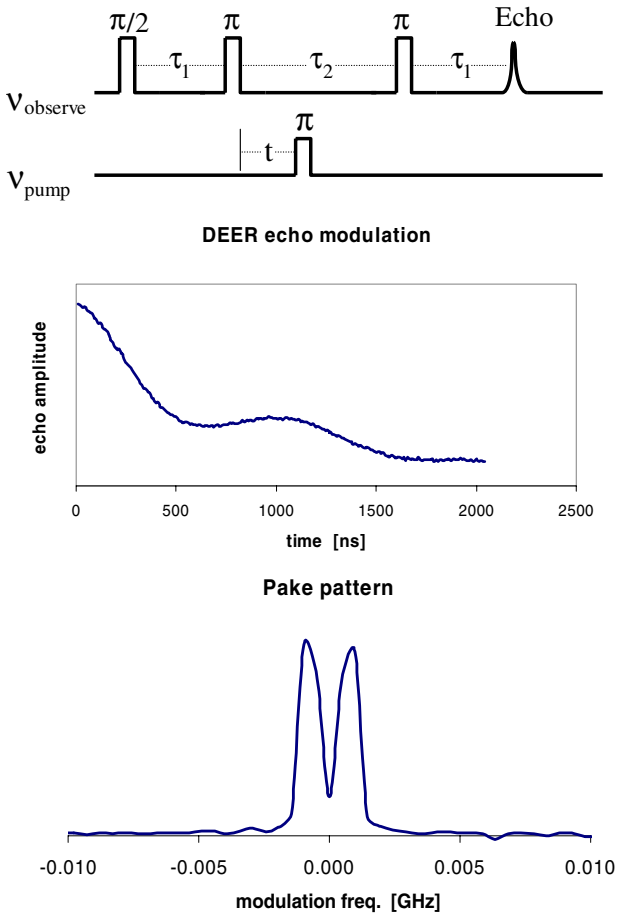

Figure 2. Double electron–electron resonance experiment (DEER). Top: the pulse sequence generates an echo corresponding to spins excited by a microwave with frequency $\nu_{observe}$; a second, pumping microwave at ν_{pump} selects another spin population. If the two populations are near each other, the dipolar field modifies the echo intensity, resulting in oscillations (middle). The time trace of the echo modulation is Fourier transformed, resulting in a 'Pake' pattern (bottom) with the splitting defined by the strength of dipolar field.

latter technique is less prone to spectral diffusion effects and it can be performed at ambient temperatures.

2.2.4. Modelling. All the techniques described above utilize spin labels that have a finite size (5–12 Å) and possess a number of single bonds (three to six) that allow for a number of rotamers. This introduces an uncertainty of the backbone–spin distance and complicates the interpretation of the spin–spin distances in terms of the protein backbone. Figure 5(A) illustrates the correlation between the $C\beta$ carbons from the x-ray structures and the spin–spin distances measured by the dipolar conventional EPR, DEER and relaxation enhancement methods in two proteins for which the atomic resolution structures are available. The correlation is particularly bad for small distances obtained by the conventional EPR method. Interspin distances of 20 Å are observed for residues with $C\beta$–$C\beta$ distance varying anywhere between 8 and 20 Å. Overall, across the whole distance range the standard deviation is ±6 Å,

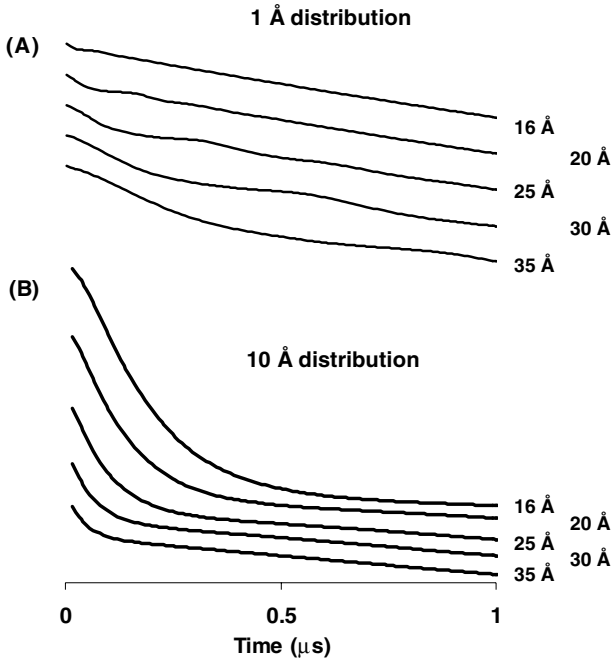

Figure 3. Sensitivity of DEER signals to increasing spin–spin separation for well defined distances (A); and in the presence of a 10 Å Gaussian distribution of distances (B).

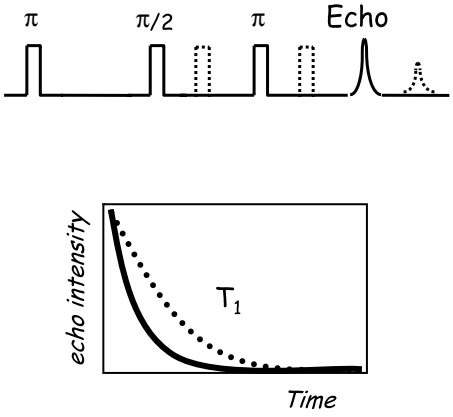

Figure 4. Inversion recovery pulse sequence measuring the spin–lattice relaxation by the decay the spin echo in the presence (solid curve) and absence (dotted curve) of the paramagnetic metal.

a tolerable error at longer distances (20–60 Å) but too large an error for short distances. This uncertainty can be improved by molecular modelling of the spin label behaviour. The modelling strategy developed in our laboratory includes Monte Carlo minimization methods to find families of lowest energy rotamers which are then used as a starting point for the molecular dynamics simulations [12]. This strategy accounts well for the tether length and rotamer structure of the spin labels, removing the aforementioned degeneracy observed at shorter distances, and reduces the standard deviation to ± 3 Å across the full distance range (figure 5(B)) [13].

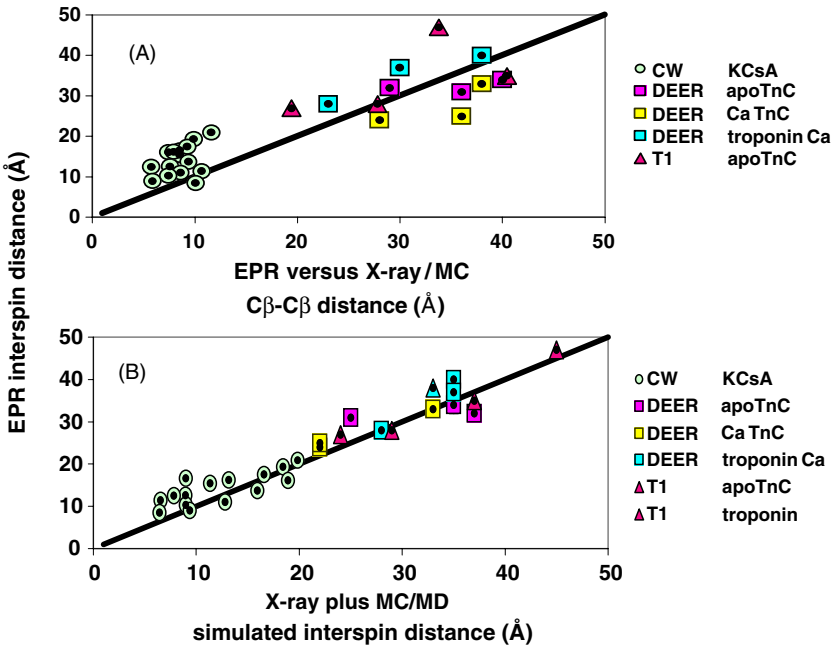

Figure 5. (A) Comparison of EPR spin–spin distances to those measured between $C\beta$ carbons. Distances measured between $C\beta$ carbons have a scatter of 6 Å when compared to the measured values. (B) Correlation between EPR distances and distances between spin labels modelled into the crystal structure using Monte Carlo and molecular dynamics methods; the scatter decreases to 3 Å and the short distances are linearized. (●) KcsA channel measured by conventional EPR; (▲) troponin C measured by relaxation enhancement by Gd^{3+}; (◙) troponin C and troponin by DEER [13].

3. Applications to muscle activation

Muscle contraction is initiated by the binding of Ca^{2+} to troponin C (TnC), a small dumbbell shaped protein consisting of N- and C-terminal lobes joined by a long α-helix. Comparison of the x-ray and NMR structures in the Ca^{2+} loaded (switched ON state) and Ca^{2+} poor states (switched OFF) reveals a movement of the C and D helices in the N-lobe that exposes a hydrophobic pocket in the Ca^{2+} bound state. Troponin C is only a calcium sensor; in muscle it forms a complex with the larger subunits troponin I (TnI), which alone is capable of inhibiting muscle force generation, and troponin T (TnT), which anchors the complex to tropomyosin which in turn transmits the signal to actin and myosin, initiating contraction. Although atomic resolution structures for isolated TnC exist, the structure of the whole complex has been determined only very recently and only in the ON state [14]. What is the troponin complex structure in solution in the OFF and in the ON states? The structure of key components that transmit the information from subunit to subunit and the nature of the involved conformational changes is the object of the spin labelling applications described below.

3.1. Site directed spin labelling

3.1.1. TnI inhibitory complex. The inhibition of force generation in muscle can be accomplished by a small segment of the TnI subunit [15]. It was postulated that this *inhibitory*

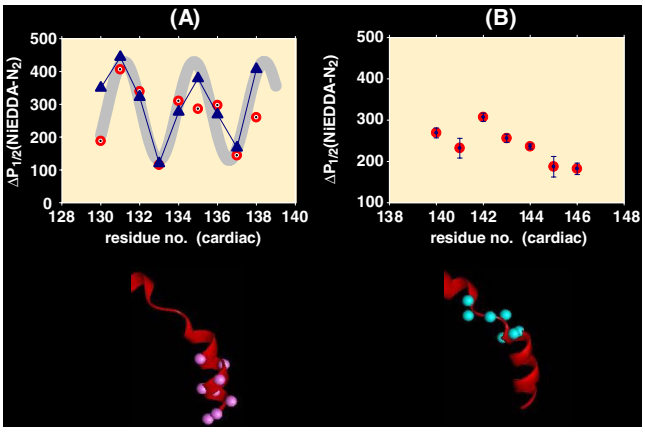

Figure 6. (A) Solvent accessibility profile for residues 130–138 of troponin I subunit. The experimental profile (•) agrees well with the profile predicted (▲) for the α-helical model proposed by homology building (below). The profile for residues 140–148; no periodicity is observed in agreement with the melted helix predicted by homology building [16].

peptide is the sensing element of TnI that responds to helix movement in the TnC subunit. Two attempts to model the structure of the TnI *inhibitory peptide* in a complex with TnC resulted in two competing models: an α-helix and a β-hairpin [16, 17]. To solve the controversy we generated single-cysteine mutants throughout the TnI *inhibitory* region and reconstituted the troponin complex with labelled TnI and unlabelled TnC and TnT subunits. The trend in accessibility to water soluble quencher (Ni-EDDA), figure 6(A), revealed a clear 3.6 periodicity for the first ten residues, indicating an α-helix. Surprisingly, this periodicity vanished for the residues at the C-terminal end of the inhibitory region, indicating a lack of defined secondary structure figure 6(B) [18]. In addition, comparison of label mobility in the complex with and without the TnT subunit revealed that the mobility in the N-terminal section of the TnI inhibitory region was strongly dampened by TnT. Such a change in residue mobility is a fingerprint of the inter-subunit interface locating TnT in the troponin complex. The dipolar distance measurements between TnI and TnC further established that TnT is sandwiched between TnC and TnI. Thus, in relatively simple experiments, cysteine scanning combined with EPR established both the secondary structure of the pivotal protein element and its location in the complex. The subsequent crystal structure of the core of the troponin complex fully verified our EPR findings [14].

3.2. Dipolar EPR

3.2.1. Troponin central helix. TnC is a member of the EF-hand protein family. Many of these undergo a large reorganization of the N- and C-terminal domains upon binding to another protein. For example calmodulin, a structural homologue of TnC, undergoes a complete 'melt' of the central helix upon binding to the myosin light chain kinase that is activated by it. The melted central helix allows for the lobes of calmodulin to wrap themselves around the target peptide. In the crystal structure of isolated TnC the helix is extended (figure 7(A)) just like in calmodulin and does not change with Ca^{2+} binding. On the other hand, the Ca^{2+} loaded crystal structure of the troponin complex reveals a melted central helix (figure 7(B)). Is this an artifact of crystal packing or does TnC change its structure only in the complex? Does Ca^{2+}

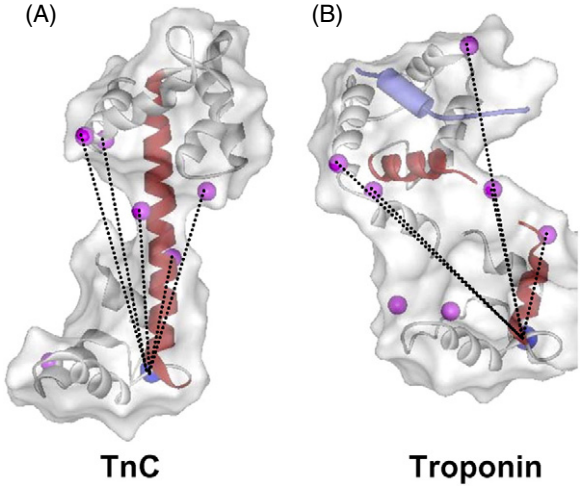

Figure 7. Conformation of the central helix of TnC (red) in the isolated subunit (A) and in the complex with troponin I and troponin T in the presence of Ca^{2+} (B). To determine the structure of the helix in the absence of Ca^{2+}, distances between the residues in the upper and lower lobes of TnC were measured in the isolated TnC and in troponin complex (dashed lines).

regulate the structure of the central helix in the troponin complex? To answer these questions we have measured the distances between the lobes of TnC in isolated and complexed forms. Paramagnetic Gd^{3+} bound at the Ca^{2+} binding sites in the C-lobe was found to decrease the T_1 relaxation time of nitroxides in the N-lobe of TnC (C12 and C51) while the distances to the central helix (C89, C94) remained unchanged. The decrease of T_1 was measured by inversion recovery and by saturation recovery [19]. Both methods indicated a major (9–11 Å) decrease of the inter-lobe distance upon complexation with other troponin subunits, consistent with bending or melting of the central helix (comparison of the crystal structures of the isolated TnC and troponin complex shows a 9 Å decrease in the distance between the probed residues). Whether the melting of the central helix is involved in muscle activation is less clear. The distances between nitroxide labels placed in the C- and N-lobes (C15/136, C15/94, C12/136) of TnC in the troponin complex changed by 5, 7 and −4 Å on addition of Ca^{2+} (DEER experiments). In isolated TnC the same distances change by −1, −8 and −6 Å (figure 8). Thus, it seems that conformational changes induced by Ca^{2+} are different in the complex and in the isolated subunit but more work on different sites is necessary.

3.3. Troponin I–N-domain movement relative to TnC C-domain

Competitive binding of the N-terminal peptide of TnI and the inhibitory peptide suggested large movement of the N-terminal peptide with respect to the C-lobe of TnC during activation. However, subsequent NMR studies suggested non-specific binding of TnI fragments to TnC, prompting us to re-evaluate this finding in the troponin complex. Nitroxides were introduced in the N-terminal portion of TnI (C51) and in the C-lobe of TnC (C100). Conventional EPR and DEER indicated a 2.5 Å increase in the inter-spin distance upon addition of Ca^{2+}, much less than expected for the displacement of the inhibitory peptide [19]. The N-terminal portion thus seems to retain its proximity to the C-lobe of TnC in the presence and absence of Ca^{2+}, consistent with its role as a structural anchor.

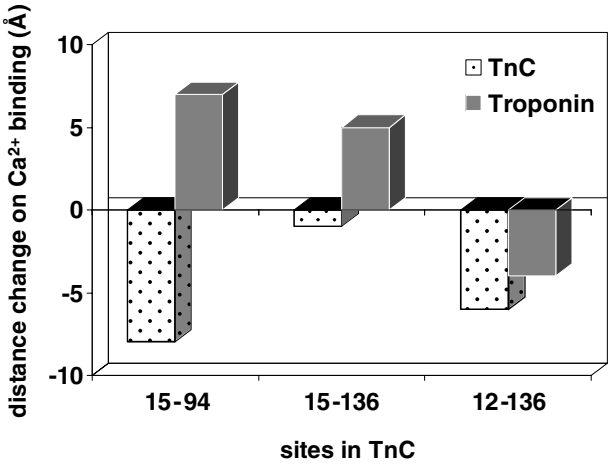

Figure 8. Changes of the inter-TnC distances induced by binding of Ca^{2+}, in the isolated subunit (*dotted*); in the troponin complex (*solid*). The changes in the troponin complex are different from equivalent conformational changes observed in the isolated subunit [19].

4. Summary

Recent advances in molecular biology and development of pulsed EPR have established EPR as a structural biology technique. Molecular biology allows introduction of spin labels at desired sites in protein structure using cysteine mutagenesis. Pulsed EPR extends the range of measurable dipolar interactions from 20 to 60–70 Å. This wide distance sensitivity range covers the dimensions of most of proteins and medium-size macromolecular complexes. The distance constraints derived from the EPR measurements can thus be used to determine the low-resolution structure of the proteins and, more importantly, follow the large conformational changes associated with biological activity.

Acknowledgments

Likai Song, Clement Rouviere and Dr Louise Brown are thanked for providing troponin data; Ken Sale was instrumental in the structural modelling of the EPR distances. The author acknowledges support from the National Science Foundation CHE-0079649 to purchase a pulsed EPR spectrometer and research grants from NSF-MCB 0346650 and the Muscular Dystrophy Association.

References

[1] Hubbell W L, Gross A, Langen R and Lietzow M A 1998 Recent advances in site-directed spin labelling of proteins *Curr. Opin. Struct. Biol.* **8** 649–56

[2] Hubbell W L, Cafiso D S and Altenbach C 2000 Identifying conformational changes with site-directed spin labelling *Nat. Struct. Biol.* **7** 735–9

[3] Fajer P 2000 Electron spin resonance spectroscopy in peptide and protein analysis *Encyclopedia of Analytical Chemistry* ed R A Meyers (Chichester: Wiley)

[4] Perozo E, Cortes D M and Cuello L G 1998 Three-dimensional architecture and gating mechanism of a K^+ channel studied by EPR spectroscopy *Nat. Struct. Biol.* **5** 459–69

[5] Rabenstein M D and Shin Y K 1995 Determination of the distance between two spin labels attached to a macromolecule *Proc. Natl Acad. Sci. USA* **92** 8239–43

[6] McHaourab H S, Oh K J, Fang C J and Hubbell W L 1997 Conformation of T4 lysozyme in solution. Hinge-bending motion and the substrate-induced conformational transition studied by site-directed spin labelling *Biochemistry* **36** 307–16
[7] Jeschke G 2002 Distance measurements in the nanometer range by pulse EPR *Chem. Phys. Chem.* **3** 927–32
[8] Milov A D, Mar'yasov A G, Samoilova R I, Tsvetkov Y D, Raap J, Monaco V, Formaggio F, Crisma M and Toniolo C 2000 Pulsed electron double resonance of spin-labelled peptides: data on the peptide-chain secondary structure *Dokl. Biochem.* **370** 8–11
[9] Pannier M, Veit S, Godt A, Jeschke G and Spiess H W 2000 Dead-time free measurement of dipole–dipole interactions between electron spins *J. Magn. Reson.* **142** 331–40
[10] Borbat P P, McHaourab H S and Freed J H 2002 Protein structure determination using long-distance constraints from double quantum coherence ESR: study of T4 lysozyme *J. Am. Chem. Soc.* **124** 5304–14
[11] Eaton S and Eaton G 2000 Distance measurements by CW and pulsed EPR *Biological Magnetic Resonance* ed L J Berliner, S Eaton and G Eaton (New York: Kluwer–Academic/Plenum) pp 2–21
[12] Sale K, Sar C, Sharp K A, Hideg K and Fajer P G 2002 Structural determination of spin label immobilization and orientation: a Monte Carlo minimization approach *J. Magn. Reson.* **156** 104–12
[13] Sale K, Song L, Liu Y, Perozo E and Fajer P G 2004 unpublished
[14] Takeda S, Yamashita A, Maeda K and Maeda Y 2003 Structure of the core domain of human cardiac troponin in the Ca(2+)-saturated form *Nature* **424** 35–41
[15] Talbot J A and Hodges R S 1981 Synthetic studies on the inhibitory region of rabbit skeletal troponin I. Relationship of amino acid sequence to biological activity *J. Biol. Chem.* **256** 2798–802
[16] Vassylyev D G, Takeda S, Wakatsuki S, Maeda K and Maeda Y 1998 The crystal structure of troponin C in complex with N-terminal fragment of troponin I. The mechanism of how the inhibitory action of troponin I is released by Ca(2+)-binding to troponin C *Adv. Exp. Med. Biol.* **453** 157–67
[17] Tung C S, Wall M E, Gallagher S C and Trewhella J 2000 A model of troponin-I in complex with troponin-C using hybrid experimental data: the inhibitory region is a beta-hairpin *Protein Sci.* **9** 1312–26
[18] Brown L J, Sale K L, Hills R, Rouviere C, Song L, Zhang X and Fajer P G 2002 Structure of the inhibitory region of troponin by site directed spin labelling electron paramagnetic resonance *Proc. Natl Acad. Sci. USA* **99** 12765–70
[19] Song L, Rouviere C, Brown L J and Fajer P G 2004 unpublished